Examining Late Twentieth Century Trends in the Central Tropical Pacific

A THESIS SUBMITTED TO
THE GLOBAL ENVIRONMENTAL SCIENCE
UNDERGRADUATE DIVISION IN PARTIAL FULFILLMENT
OF THE REQUIREMENTS FOR THE DEGREE OF

BACHELOR OF SCIENCE

IN

GLOBAL ENVIRONMENTAL SCIENCE

MAY 2015

By

Ted Conroy

Thesis Advisor

Professor Brian Powell

I certify that I have read this thesis and that, in my opinion, it is satisfactory in scope and quality as a thesis for the degree of Bachelor of Science in Global Environmental Science.

_____

Professor Brian Powell
Department of Oceanography

Acknowledgements

Abstract

Examining Late Twentieth Century Trends in the Central Tropical Pacific. Ted Conroy, May 2015. University of Hawaii at Manoa. Coral Proxy records are key to understanding the El Niño Southern Oscillation (ENSO) prior to the observational era. This study investigates how coral proxy records have captured changes over the late twentieth century, the most observational rich time period in history. An isotope enabled regional ocean modeling system (isoROMS) was used for this study, and allows for oxygen isotopic ratios (δ^{18}O) to be calculated and directly compared to corals. Results show that Sr/Ca ratios record sea surface temperature trends well; however, a nonlinear relationship between sea surface salinity and seawater δ^{18}O complicates paleo-salinity measurements. Also, late twentieth century warming and freshening trends in the central tropical Pacific appear to be strongly influenced by decadal changes that must be identified to understand long term anthropogenic effects.

Table Of Contents

List of Figures

Chapter 1: Introduction

   The Tropical Pacific Ocean is a highly dynamic region characterized by the interaction between the ocean and atmosphere. The strong variability between the two is the El Niño Southern Oscillation (ENSO) that has implications for global temperature and precipitation. ENSO alters the east to west gradient of sea surface temperatures (SST) with resulting changes occurring in the overlying atmosphere. The ENSO cycle affects ecosystems, agriculture, rain patterns, hurricanes, and other severe weather events (Collins et al., 2010), which make it pertinent from a societal perspective. The dynamics of ENSO have been characterized, but as humans alter the climate system through fossil fuel burning, future changes to ENSO are not well constrained, and could have a significant impact on the global climate system. Future ENSO predictions are estimated using a variety of Global Climate Models (GCM), and scenarios vary between studies. In order to understand changes to future ENSO variability and strength, knowledge of past natural ENSO variability is required.

   Observations from the tropical Pacific Ocean are critical to understanding ENSO dynamics as well as fluctuations in past ENSO variance. The late twentieth century (1980-present) is observationally rich thanks to satellites; however, there are very few observations before 1980. It has been shown that in order to understand the ENSO process, much longer observational time periods

are needed: on the order of 250 years (Stevenson et. al, 2010). Without direct measurements, proxy records must be used to extend the observational record in the Tropical Pacific Ocean. The stable oxygen isotope record found in coral skeletons may be well suited for ENSO reconstruction.

Changes in the oxygen isotope ratio of $^{18}O/^{16}O$ ($\delta^{18}O$) in corals correspond to changes in sea surface temperature and the $\delta^{18}O$ of the seawater. During coral growth, the $\delta^{18}O$ of the surrounding seawater is "recorded", as the fractionation during calcium carbonate precipitation depends on temperature. Seawater $\delta^{18}O$ ($\delta^{18}O_{sw}$) is commonly assumed to be linearly correlated with sea surface salinity (Nurhati et. al, 2009). However, the linear relationship assumed between $\delta^{18}O_{sw}$ and sea surface salinity may not be a good approximation. In nature, the true relationship is nonlinear, and other factors can affect the $\delta^{18}O$ of the coral.

Multiple studies have used corals to infer past Tropical Pacific climate changes, such as Cobb et. al(2003), Nurhati et. al(2009), and Carilli et. al(2014). In particular, Nurhati et. al (2009) examined over 25 years (1972-1998) of coral data from the Line Islands, in the central tropical Pacific Ocean. Strong negative trends in coral $\delta^{18}O$ were seen, and Nurhati et. al (2009) concluded that the region has been getting warmer and wetter. Strontium/Calcium (Sr/Ca) ratios suggest both that warming has increased towards the equator and a decrease in equatorial upwelling (Nurhati et. al, 2009). In this study, trends from coral proxy

records are investigated throughout the central Tropical Pacific. Because of the

sparsity of Pacific Island coral records, model reconstructions of the Pacific Ocean

can help to understand spatial $\delta^{18}O$ patterns, and how well the ocean basin

patterns correlate to specific Islands where the coral records are from. The goal

of this work is to understand if $\delta^{18}O$ coral data can describe the ocean, such as

sea surface and subsurface temperature, sea surface salinity, and to assess claims

made by using coral $\delta^{18}O$ data. Using an isotope enabled numerical model of

the tropical Pacific Ocean, it is possible to evaluate regional variation, and to see

if trends that coral records show are present in the model over the most

observational rich time period in history.

Chapter 2: Background

The ENSO cycle operates on a 2-7 year inter-annual period. The Western Pacific is characterized by warm SSTs, with a deep thermocline as a result of the large volume of warm water on the surface, that converged as a result of the trade winds pushing water to the west. In contrast, the Eastern Pacific is characterized by a shallow thermocline, as a result of the regional upwelling caused by the regular easterly trade winds. As a primary driver of ENSO, the Walker circulation is the zonal atmospheric flow over the tropical Pacific. The Walker circulation is due to the large heat loss into the tropical atmosphere that leads to convection of warm and wet air. As the air is lifted into the atmosphere, rain will fall out, and this colder and drier air moves east, eventually downwelling in the Eastern Pacific. There are several distinct phases of ENSO: the warm phase, referred to as El Niño, and cold phase, La Niña, and the neutral phase. During neutral conditions, the equatorial tropical Pacific is characterized by a large zonal subsurface temperature gradient, as a result of the dominant easterly trade winds. El Niño is characterized by anomalously warmer sea surface temperatures (SSTs) in the central and eastern equatorial Pacific, as well as enhanced convective rainfall and below average air pressure in the central and eastern equatorial Pacific. Westerly wind bursts initiate the movement of warm water towards the eastern end of the basin, in the form of downwelling Kelvin

waves. As a result of a weakened Walker circulation, a decrease in upwelling in

the Eastern Pacific can be observed during El Niño events, associated with

reduction of easterly trade winds. La Niña events occur from the return of

strengthened easterly trade winds, as they are essentially an intensification of

neutral conditions. Enhanced trade winds strengthen upwelling on the eastern

boundary, which shoals the thermocline in the eastern Pacific. La Niñas are

associated with cooler than normal sea surface and subsurface temperatures in

the central and eastern Pacific, and enhanced warming and convection in the

western Pacific.

Changes to the climate system by anthropogenic warming are important

to understand, especially for ENSO. The future global warming scenario in the

Tropical Pacific, characterized by Collins et. al (2010), is expected to change the

mean state of the ocean, while future ENSO activity is not fully understood.

Most coupled models predict that changes in the mean state will be manifested

as a weakening of the easterly trade winds, a decrease in atmospheric convective

flux (Held and Soden, 2006), and SSTs warming fastest near the equator but more

slowly in other regions. The equatorial thermocline is expected to shoal, and the

temperature gradients across the thermocline are expected to become steeper.

McPhaden and Zhang (2002) find a reduced overturning circulation between the

tropics and the subtropics since 1970, which caused a decrease in upwelling in

the equatorial region from 9°N-9°S. The equatorial upwelling is supplied by cold, higher latitude water. Because this pattern is similar to the projected trends for a warmer climate, shown by Collins et. al (2010), it is possible that the recent climate fluctuations have been influenced by both global warming and natural variability. However, McPhaden and Zhang (2002) note that it is not possible to separate the effects of anthropogenic warming on the climate system using short data records. Many studies have investigated this topic, including Vecchi et. al (2006), who show a weakened Walker circulation, using a long record of the Southern Oscillation Index (SOI), and suggest this is due to anthropogenic forcing. Using a 155 year coral record, Urban et. al (2000) found that two thirds of the negative trend was due to the period after 1976, and that the trend was unprecedented since the record began in 1840. They suggest an anthropogenic shift in the late twentieth century. Tokinaga et. al (2012) find a slowdown of the Walker Circulation from 1959-2009, associated with SST warming patterns and reduced zonal gradients. Williams et. al (2010) find a shoaling of the thermocline in the Western Pacific, which supports the reduction of the Walker Circulation in the twentieth century. In contrast, Karnauskas et. al (2009) suggest that the Pacific zonal SST gradient has strengthened from 1880-2005. Since the late 1990's, dissimilar conditions have been prevalent in the Tropical Pacific. England et. al (2014) shows strengthening of Pacific trade winds accounts for cooling of the

tropical Pacific, and is related to the slowdown in surface warming globally. This has caused increased equatorial upwelling in Eastern & Central Pacific, and is associated with the global warming hiatus.

The late twentieth century encompasses the satellite era, the implementation of the Tropical Atmosphere Ocean (TAO) array, and more recently, the drifting ARGO profiling floats. Prior to the 1980's, observational data was obtained from ship-board measurements, which are limited spatially to shipping routes, and are on various time scales as well. These data would be compiled and interpolated onto a grid at distinct times. This leads to obvious errors, but remained the best option for assessing patterns over time. After the strong 1982 El Niño, the need for i*n situ* data collection in the region was recognized, which sparked the installation of the Tropical Atmosphere Ocean Array (TAO) (McPhaden et. al, 1998), which has been continuously collecting data since. This is also the time period when satellites began to provide large amounts of data, allowing for the late twentieth and the early twenty-first centuries to be well observed compared to previous times for this region. Various indices have been created in order to measure the ENSO cycle, including the Niño 3.4 Index, the Ocean Niño Index (ONI), and the Southern Oscillation Index (SOI). In this study, the Niño 3.4 Index and ONI will be used. The Niño 3.4 Index is the average SST of the Niño 3.4 region (5°N-5°S, 170°-120°W), which

is a key region for ENSO variability, and is able to show ENSO events and amplitude. The ONI is similar to the Niño 3.4 index, but is the climatological anomaly for each month of the year. The resulting ONI is either positive during El Niño events or negative during La Niña events, and the magnitude of the anomaly corresponds to the strength of the event.

In order to reconstruct climate prior to the era of instrumental and satellite data, the coral proxy data must be used. The isotopic ratio of stable oxygen isotopes $^{18}O/^{16}O$, referred to as $\delta^{18}O$, found in skeletal coral is commonly used for ENSO reconstruction. Skeletal coral $\delta^{18}O$ is used as a proxy for sea surface temperature and the $\delta^{18}O$ of the surrounding seawater, since variability of $\delta^{18}O$ from corals arises from the temperature, as well as the $\delta^{18}O_{sw}$ (Grottoli et. al, 2007). As the temperature increases, the precipitate coral $\delta^{18}O$ decreases, due to temperature dependent fractionation effects, creating an inverse relationship between SST and coral $\delta^{18}O$. The fractionation yields a slope for the SST/coral $\delta^{18}O$ relationship of approximately -0.2 (Russon et. al, 2013). Changes in $\delta^{18}O_{sw}$ reflect proportional changes in coral $\delta^{18}O$, as increasing $\delta^{18}O_{sw}$ will increase coral $\delta^{18}O$. Rainwater in the tropical Pacific is $\delta^{18}O$ depleted relative to seawater: a result of heavier isotopes being preferentially precipitated and accumulated in the seawater. During precipitation events, $\delta^{18}O_{sw}$ therefore decreases, because the precipitation is more negative than the seawater. More negative coral $\delta^{18}O$

anomalies are thus associated with warmer and wetter conditions and positive

anomalies are associated with colder and drier conditions (Stevenson et. al, 2013).

It is possible for the effects of temperature and precipitation to cancel each other

out, and other influences such as runoff and smaller scale processes can also

affect coral $\delta^{18}O$. While $\delta^{18}O_{sw}$ is correlated with the sea surface salinity, the

relationship between the two varies with latitude, depth, ocean basin, and

regional factors that determine $\delta^{18}O_{sw}$ (LeGrande and Schmidt, 2006).   The coral

$\delta^{18}O$ signature is a mixture of the $\delta^{18}O_{sw}$ and SST signals, and the coral $\delta^{18}O$

signal can be biased either by SST or $\delta^{18}O_{sw}$ because the variance of coral $\delta^{18}O$ is

dependent on the covariance of $\delta^{18}O_{sw}$ and SST. For instance, in the western

tropical Pacific, where there is a very active hydrological cycle, the $\delta^{18}O_{sw}$ signal

may dominate the coral $\delta^{18}O$ record, leaving little trace of the SST signal in the

coral $\delta^{18}O$ record. One way to separate the SST and coral $\delta^{18}O$ is by also using

strontium and calcium ratios, which are a separate proxy record of SST, and then

to remove the SST influence from the coral $\delta^{18}O$, resulting in a $\delta^{18}O_{sw}$ record

(Nurhati et. al, 2009).

In order to accurately quantify coral $\delta^{18}O$ variations, linear functions have

been developed, termed pseudocorals, that are able to relate coral $\delta^{18}O$ to SST

and sea surface salinity (SSS) directly. Pseudocoral approximations allow for

coral $\delta^{18}O$ data to be interpreted as linear changes in SST and SSS, giving relevant

estimates of past climate variables. However, these linear assumptions aren't as simple in nature. Stevenson et. al (2013) showed that errors associated with using pseudocorals are on the order of 37-75% of coral $\delta^{18}O$ variance. Pseudocorals have large errors as a result of the complexity of $\delta^{18}O_{sw}$, and the linear assumption leads to large errors in the variance estimate of coral $\delta^{18}O$ (Stevenson et. al, 2013). $\delta^{18}O_{sw}$ is modified by changes to advection, changes to water mass properties, the relative amounts of precipitation and evaporation, and precipitation $\delta^{18}O$ values (Stevenson et. al, 2013).

To estimate changes in past SSS, linear "calibration" slopes are developed from paired $\delta^{18}O_{sw}$ and SSS measurements. Unfortunately, these linear calibration slopes are typically not derived from the study site, as paired $\delta^{18}O_{sw}$ and SSS measurements are extremely sparse (Stevenson et. al, 2013). This results in large errors in the calculated slope. LeGrande and Schmidt (2006) derive basin averaged $\delta^{18}O_{sw}$/SSS slopes of 0.27 ‰ practical salinity unit (psu) for the Tropical Pacific. Using the Legrande and Schmidt (2006) linear calibration slopes along with instrumental SST and SSS for reconstructing coral $\delta^{18}O$ variance, Stevenson et. al (2013) demonstrated that the linear relationship between $\delta^{18}O_{sw}$ and SSS is unable to reproduce the coral $\delta^{18}O$ variability. $\delta^{18}O_{sw}$, as observed in corals, is controlled by advection, changes to water mass properties, by amounts of precipitation and evaporation, and local $\delta^{18}O$ of precipitation (Stevenson et. al,

2013). Model studies have shown that the $\delta^{18}O_{sw}$/SSS relationship likely varies

with time as well (LeGrande and Schmidt, 2011). Longer time periods are

needed in order to determine the relationship. Numerical models, such as the

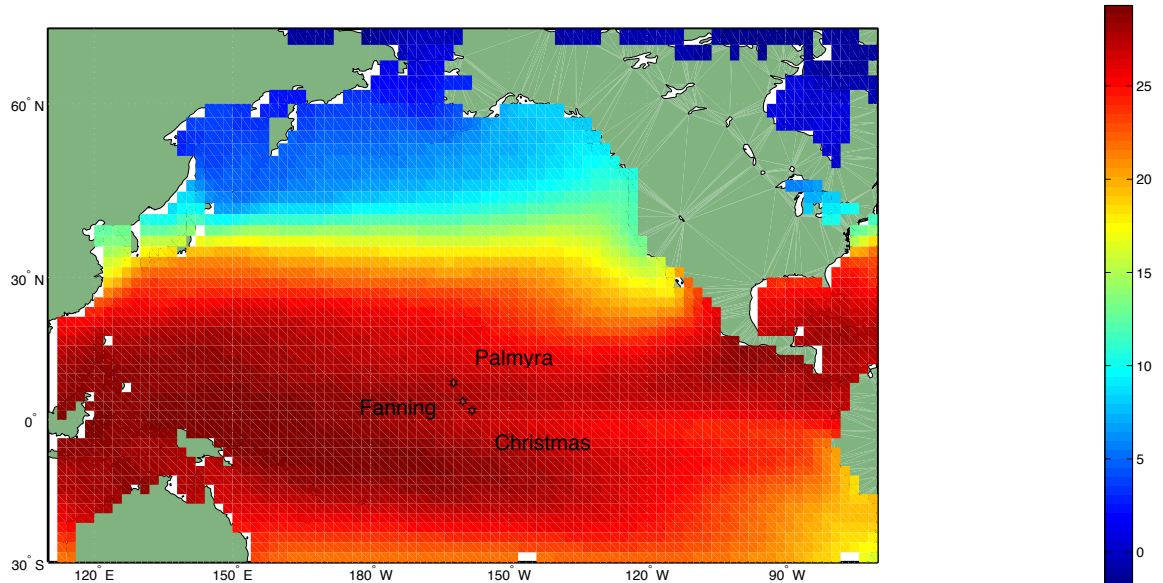one used in this study, may be able to analyze the $\delta^{18}O_{sw}$: SSS relationship.

Figure 1. Map of study region & average sea surface temperature (°C)
from Extended Reconstruction of Sea Surface Temperature (ERSST) v.3b,
1972-1998.

Multiple studies have been performed using coral $\delta^{18}O$ to reconstruct

climatic conditions in the tropical Pacific. Using all coral $\delta^{18}O$ data, Grottoli et. al

(2007) showed warming trends in the Pacific from 1860-1990 of about 0.79 °C.

Carilli et. al (2014) have compiled $\delta^{18}O$ coral records from across the Tropical

Pacific from 1959 to 2010. Using sites in the western and central equatorial

Pacific, $\delta^{18}O$ and Sr/Ca data show a reduction in the zonal SST and SSS gradient

11

between these regions, implying a weakening in the Walker circulation. From

the coral data, the Gilbert Islands, in the Western Pacific, have warmed in the

time period at a slower rate than the Line Islands, in the reported by Nurhati et.

al (2009). In addition, little freshening has occurred in the Gilbert Islands,

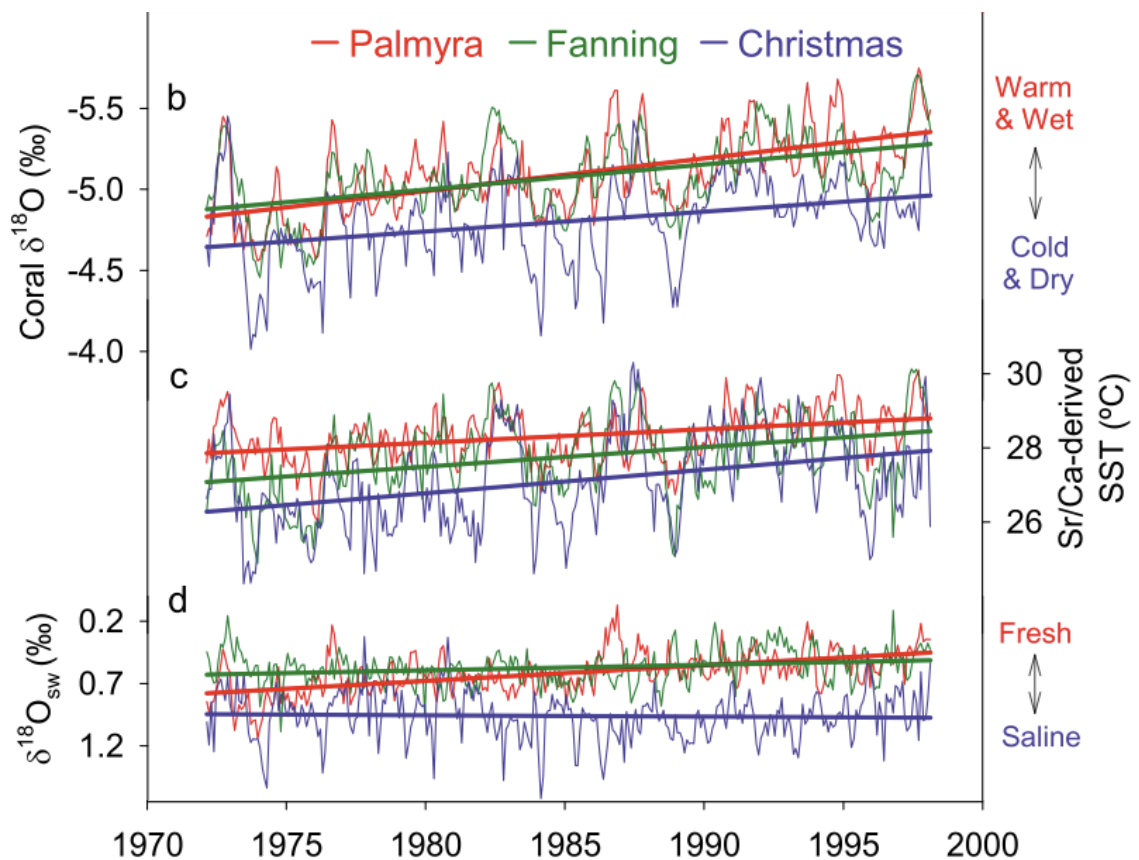compared to freshening indicated by reduced δ18O seawater in the Line Islands.

Figure 2. Coral proxy data from Nurhati et. al (2009).

Using coral proxy records, Nurhati et. al (2009) show trends in the Line

Islands over the late twentieth century from 1972-1998. The Line Islands have

been used extensively for ENSO reconstruction, due to their location and

12

availability of coral $\delta^{18}O$ data (Cobb et. al 2001, 2003, 2013, Nurhati et. al 2009,2011). The Line Islands (shown in Figure 1), specifically Palmyra Atoll, Fanning Island, and Christmas Island, are relevant because they are found in the Niño 3.4 region, and are aligned in a north to south order, giving a meridional component to the $\delta^{18}O$ records. Palmyra's location is in the path of the North Equatorial Counter Current (NECC), and its rainfall is associated with the Inter-Tropical Convergence Zone (ITCZ). Furthest south, slightly north of the equator, Christmas Island is influenced by equatorial upwelling, and has cooler waters than Palmyra and Fanning to the north (Nurhati et. al, 2009). Nurhati et. al (2009) found strong negative coral $\delta^{18}O$ trends in the Line Islands from 1972-1998 as shown in Figure 2. The coral $\delta^{18}O$ trends are -0.52 ± 0.09(‰/26yr) at Palmyra, -0.40 ± 0.09(‰/26yr) at Fanning, and -0.32 ±0.10(‰/26yr) at Christmas Island. Sr/Ca ratios were also used as a proxy for SST and show warming trends that increase towards the equator. Nurhati et. al (2009) associate this with a decrease in equatorial upwelling. Using coral $\delta^{18}O$ and removing the SST component with Sr/Ca ratios, $\delta^{18}O$ seawater records from Palmyra, Fanning, and Christmas exhibit trends over the entire period of -0.32 ± 0.08(‰/26yr), -0.12 ± 0.08(‰/26yr), 0.03 ± 0.11(‰/26yr), respectively. More negative $\delta^{18}O_{sw}$ trends on the southern edge of the ITCZ are suggested to be a result of the strengthening and/or an equatorward shift of the convergence zone (Nurhati et. al, 2009). Nurhati

et. al (2009) stress that these trends favor "El Niño like" conditions in the tropical

Pacific, and that these changes are a result of anthropogenic forcing. However,

most significantly, Nurhati et. al (2009) used a $\delta^{18}O$ time series that ended at the

peak of the largest ENSO event on record, which may strongly bias their results.

Stevenson et. al (2015) quantifies mesoscale processes which have an effect

on coral $\delta^{18}O$ variability in the Line Islands, using the same numerical model in

this study. In Palmyra, tropical instability waves produce temperature

excursions of up to 1 °C during boreal winter and La Niña events. Christmas

Island is most affected by fronts with Island topography to create SST offsets

between opposite sides of the Island, suggesting differences from coral $\delta^{18}O$

throughout the Islands are due to physical oceanographic effects. Stevenson et.

al's (2015) work shows that the relationship between SSS and $\delta^{18}O_{sw}$ becomes less

correlated at higher resolution, due to small scale processes affecting SST, SSS,

and $\delta^{18}O_{sw}$ differently. This study focuses upon the Line Island study by Nurhati

et. al (2009), in attempt to validate coral proxy records as well as extend the coral

$\delta^{18}O$ record beyond the study of Nurhati et. al (2009).

Chapter 3: Methods

This study encompasses the central Tropical Pacific Ocean, with a focus on the Line Islands, in the central equatorial region of the Pacific Ocean, as shown in Figure 1. The Line Islands are located from 2°N – 6°N, 157°W – 162°W, in the Niño 3.4 region, that is used for measuring ENSO variability.

Chapter 3.1: isoROMS

This study was performed using an isotope enabled Regional Ocean Modeling System (isoROMS), a modified version of ROMS (Shchepetkin and McWilliams, 2005) to which oxygen isotopes were added by Stevenson et. al (2015). IsoROMS is capable of simulating changes in $\delta^{18}O$ by adding $H_2^{16}O$ and $H_2^{18}O$ as passive tracers in the water column. For boundary and initial conditions for isoROMS, Stevenson et. al (2015) used the German Contribution to the Estimating of the Circulation and Climate of the Ocean (GECCO2) for oceanic conditions, the global gridded dataset from LeGrande and Schmidt (2006) for seawater oxygen isotopes, and the Common Ocean-Ice Reference Experiment (CORE2) for atmospheric forcings. The atmospheric forcing contains only climatological precipitation data prior to 1979; therefore, the study period for isoROMS has been restricted to 1979-2009. The model has a variable spatial resolution with less than fifty kilometers for the Islands of interest, much finer than prior GCM experiments that have been used for isotope simulations.

From isoROMS output, $\delta^{18}O$ of seawater can be calculated using:

$$\delta^{18}O_{seawater} = \left(\frac{\left(\frac{^{18}O}{^{16}O} \right)_{sample}}{\left(\frac{^{18}O}{^{16}O} \right)_{standard}} - 1 \right) * 1000\%o$$

The Vienna Standard Mean Ocean Water (VSMOW) is used for the $\delta^{18}O_{sw}$

standard. For direct comparison with $\delta^{18}O$ from corals at the Line Islands, we

must convert the seawater value to coral value by:

$$\delta^{18}O_{coral} = \delta^{18}O_{seawater} - \alpha T$$

where T is the bulk temperature of the model, and the bulk $\delta^{18}O$ of seawater is

used. Bulk values, the average of the shallowest 50 meters of the grid cell, were

computed for temperature, salinity, and $\delta^{18}O$ in order to better represent the

upper water parcel. For this study, α of 0.22 was used (Russon et. al, 2013).

Chapter 3.2: Model Validation

Model comparisons and validations were done with the following data

sources: 1) Extended Reconstruction Sea Surface Temperature v3.b (ERSST)

(Smith et. al, 2008) for SST; 2) gridded SSS product from Delcroix et. al, 2011;

3) Nurhati et. al (2009) for the Line Islands coral $\delta^{18}O$ data; and 4) TAO array for

20 °C isotherm (McPhaden et. al, 1998). Model validations were performed for i)

the Niño 3.4 index (Figure 3), ii) the Ocean Niño Index (ONI) (Figure 4), iii)

Palmyra, Fanning, and Christmas Island SST (Figure 5), iv) Palmyra, Fanning,

and Christmas Island SSS (Figure 6), v.) the 20 °C isotherm depth (Figure 7), and

vi.)Palmyra, Fanning, and Christmas Island $\delta^{18}O$ coral (Figures 8-10).

Correlation coefficients are used (R-value) for Figures 3-6 and 8-10 to show how

well the model captures the variability. The bias value is the mean of the model

subtracted by the mean of the observed data, to provide an estimate of the offset

of the two. IsoROMS was integrated over the time period of 1979-2009, while

Nurhati et. al (2009) used the time period of 1972-1998 for $\delta^{18}O$ of corals in the

Line Islands. This provides nearly twenty years of direct comparison.
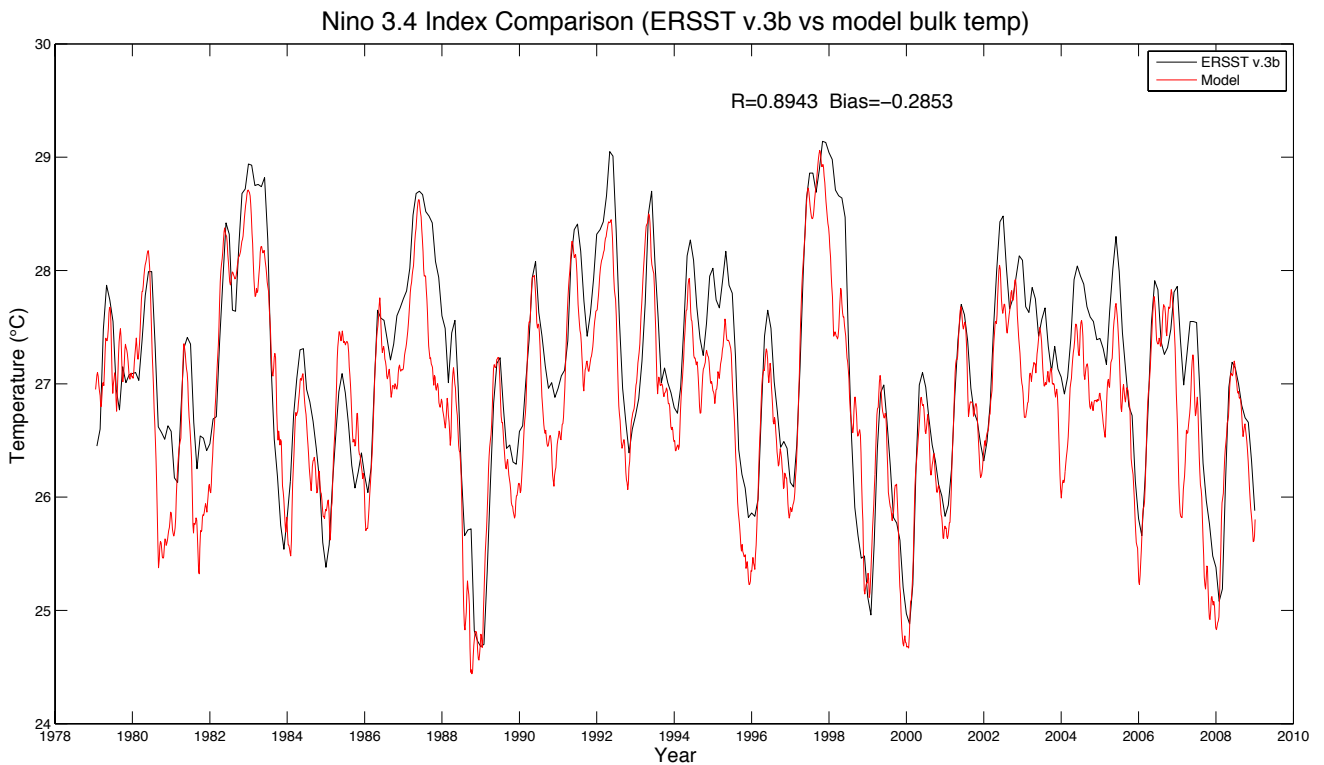
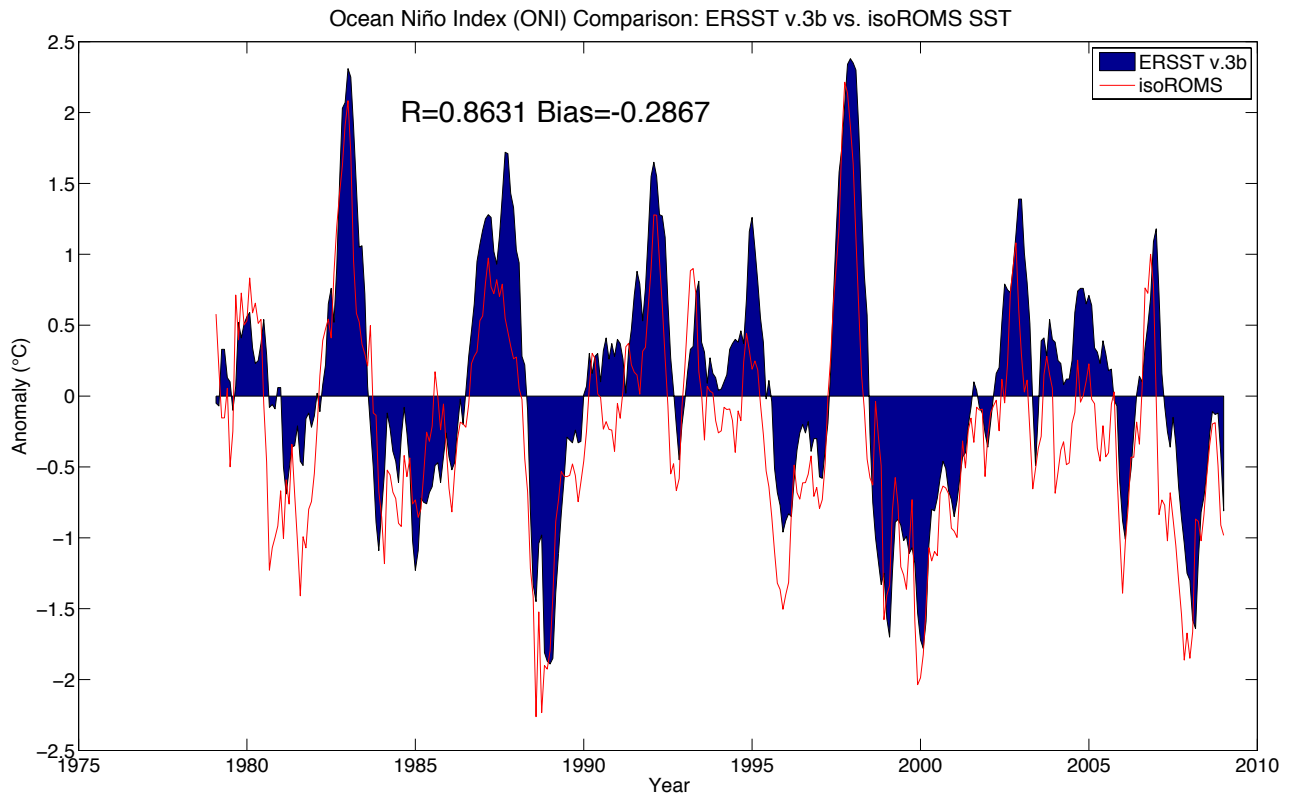Figure 3. Nino 3.4 Index Comparison.

Figure 4. Ocean Nino Index (ONI) comparison. Climatological means from ERSSTv.3b were used for isoROMS calculations.

The model does very well in replicating sea surface temperature, as seen

in the Niño 3.4 Index comparison (Figure 3), the ONI comparison (Figure 4),

shows that isoROMS and the Line Islands SST comparisons (Figure 5). IsoROMS

is able to simulate ENSO variability as well as the strong El Niño and La Niña

events, as seen in Figure 3 and Figure 4. For the Line Islands, R-values for SST

are 0.8249, 0.8055, and 0.8323, for Christmas, Fanning, and Palmyra, respectively.

IsoROMS salinity comparison (Figure 6) to the gridded SSS data set from

Delcroix et. al (2011) is not as well simulated, with R-values of 0.1061, 0.0315,

and 0.0272, for Christmas, Fanning, and Palmyra, respectively. However, the

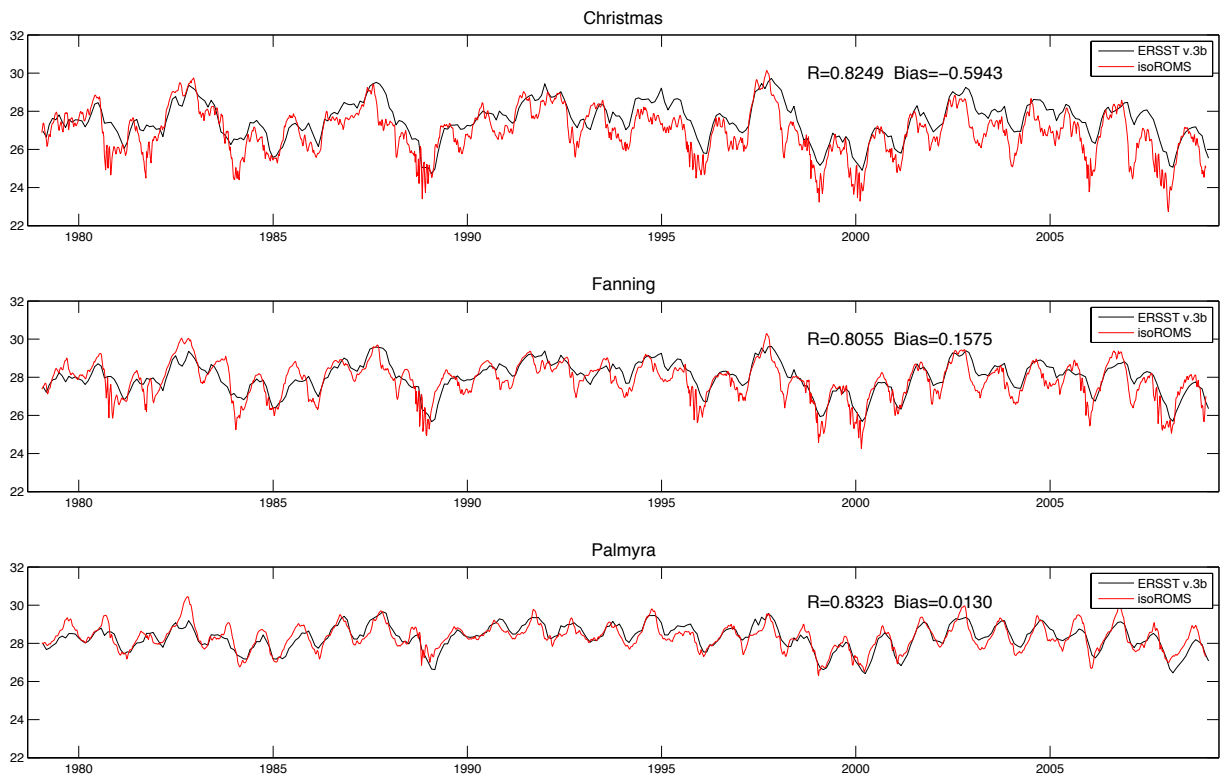model is in the same range as the observational data, as seen by the bias.

18

Figure 5. SST comparisons. ERSST v.3b, in black, and isoROMS, in red. Bulk temperature (50m) are shown for isoROMS.
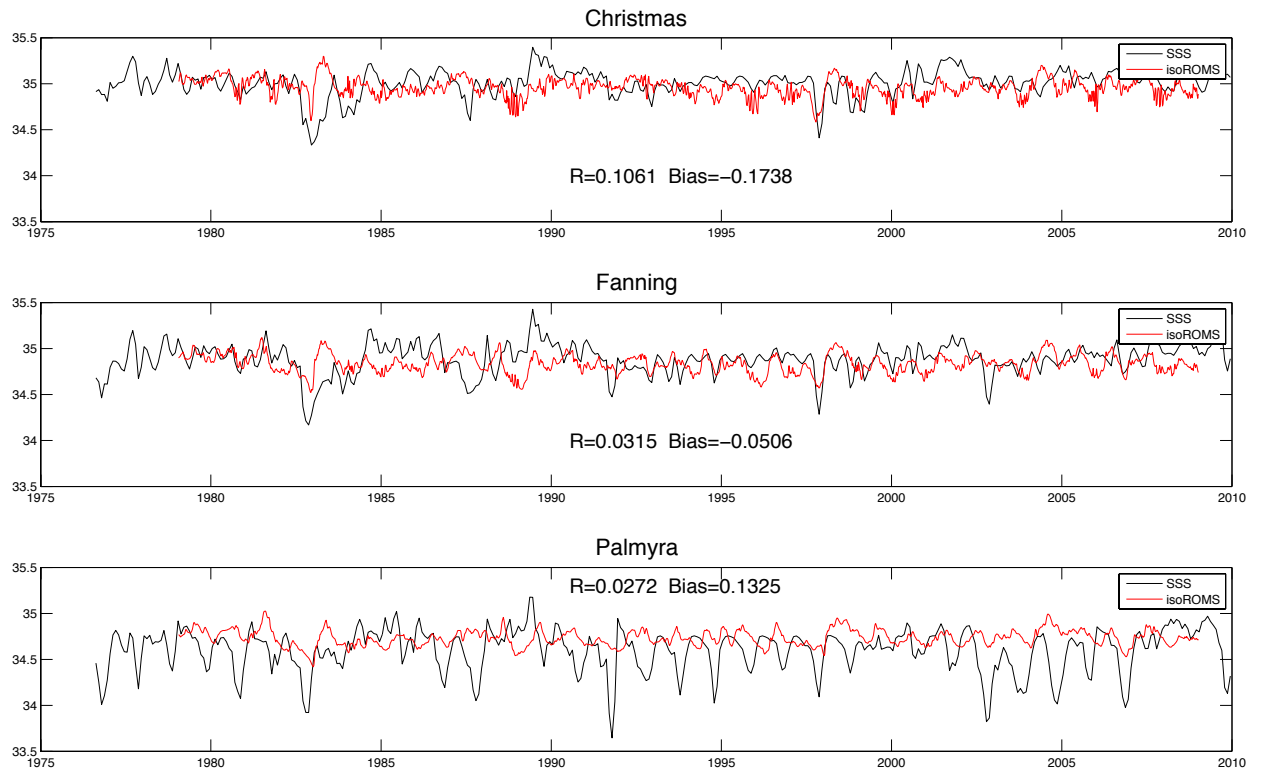

Figure 6. Sea surface salinity comparison. Gridded SSS data from Delcroix et. al (2011), in black, and isoROMS, in red, are shown. IsoROMS data is comprised of bulk salinity (50m).

Stevenson et al. (2015) calculate that the root mean squared error shows the differences between GECCO2 and isoROMS was less than those between GECCO2 and Delcroix et. al (2011). Because of the significant errors between various data sets, isoROMS salinity is as valid as the others to consider; however, the uncertainties are large.
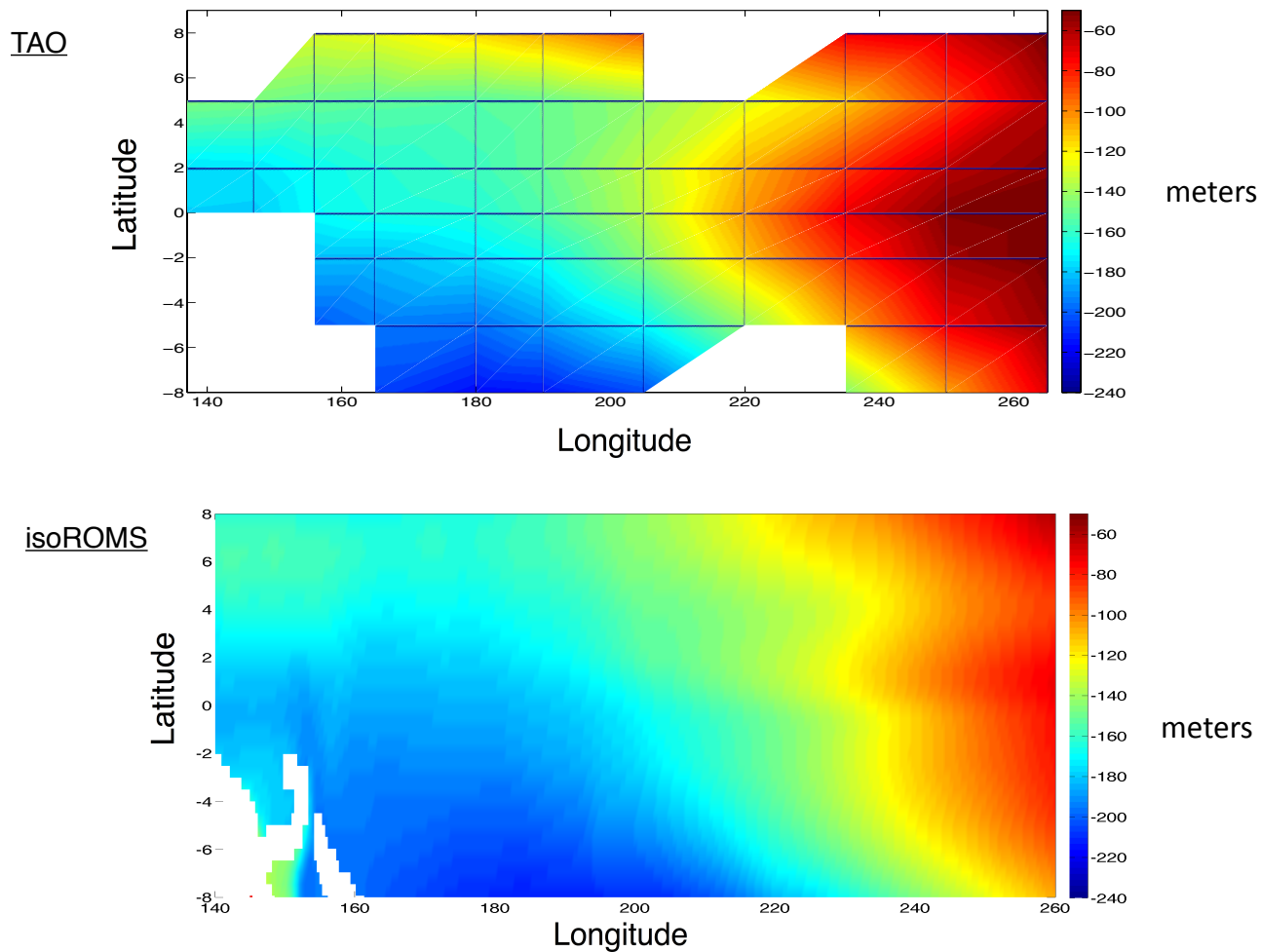

Figure 7. Comparison of TAO & isoROMS mean depth of 20 °C isotherm (meters). TAO is upper plot and isoROMS is lower plot.

Thermocline depth is an important factor in the Tropical Pacific, as the east-west thermocline gradient is a significant component of ENSO. The TAO

array provides subsurface temperatures in the region from 1990 onward, providing for some degree of validation for the model. The common method of defining the thermocline in the Tropical Pacific is the depth of the 20°C isotherm.The thermocline is defined as where the greatest vertical gradient of temperature is located (dT/dz). For this project, both the 20 °C isotherm and dT/dz were calculated from the model, while the 20 °C isotherm was taken from the TAO array for comparison. The dT/dz method and the 20 °C isotherm are found to be almost identical, with the dT/dz method showing slightly stronger trends in both shoaling and deepening.

We define a a seasonally resolved linear regression by:

$$regression = y_0 + mt + A_0 \sin\left(\frac{2\pi}{365.25}t\right) + A_1 \cos\left(\frac{2\pi}{365.25}t\right)$$

The trends were computed for various indices and periods of time from both observational data and model output. The regression was used in order to remove seasonal signals from the trends, leaving longer term signals of interest for this study. Interpolation was used for comparing the model with observational data to obtain an R-value for the two data sets. For all analyses, interpolation was solely used to find the R-value, and the plots are comparisons of the original data and isoROMS.

For Palmyra, Christmas, and Fanning Island, a three by three grid cell box was used for isoROMS for comparisons in the Line Islands, resulting in a box

that is roughly one degree in size, comparable to gridded SST and SSS products.

Using equation 2, coral $\delta^{18}O$ is calculated from SST and $\delta^{18}O_{sw}$ from the model. $\delta^{18}O_{sw}$ is calculated using bulk $H_2^{16}O$ and $H_2^{18}O$. As shown in Figures 8-10, correlation between coral $\delta^{18}O$ and modeled coral $\delta^{18}O$ are good, with R-values of 0.54, 0.62, and 0.62 for Christmas, Fanning, and Palmyra, respectively, and the model is able to reproduce the inter-annual variability of $\delta^{18}O$ seen in corals. Trends for both coral $\delta^{18}O$ and isoROMS are shown for each Island. The magnitude of trends are in disagreement over the common period of 1979-1998, but they both show decreasing $\delta^{18}O$. Trends for the overlapping period of coral $\delta^{18}O$ are -0.36(‰/20yr) and -0.53(‰/20yr), compared with isoROMS of
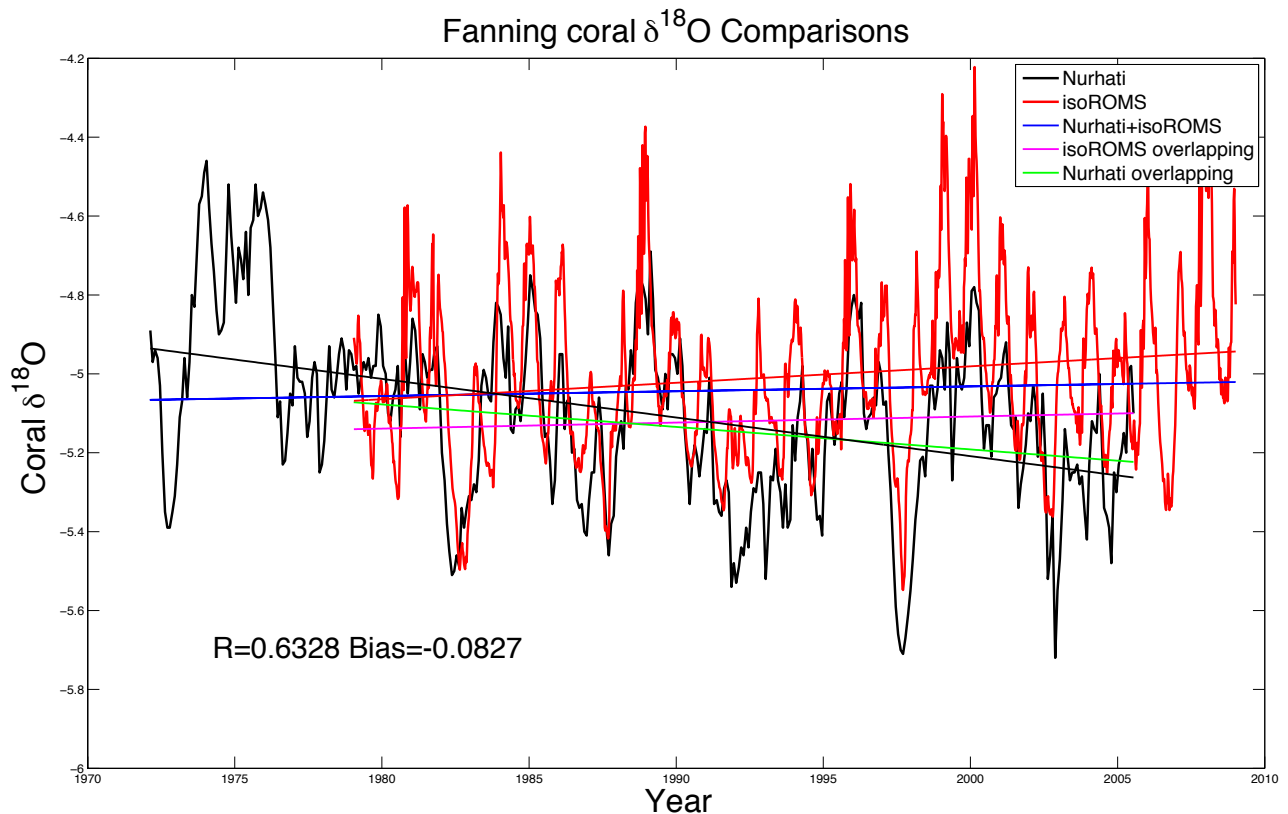

Figure 8. Fanning Island coral $\delta^{18}O$ (‰) comparison.

Figure 9. Palmyra Atoll coral δ¹⁸O (‰) comparison.
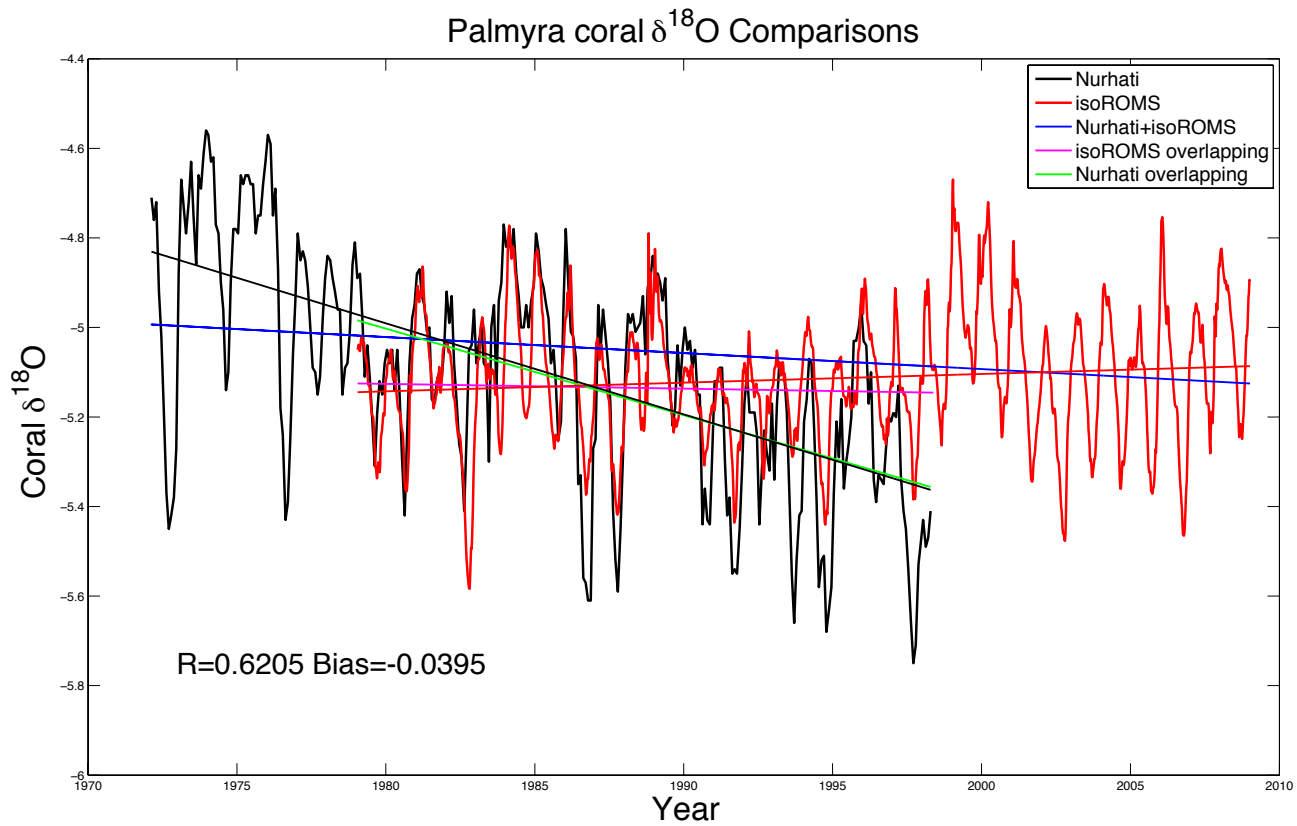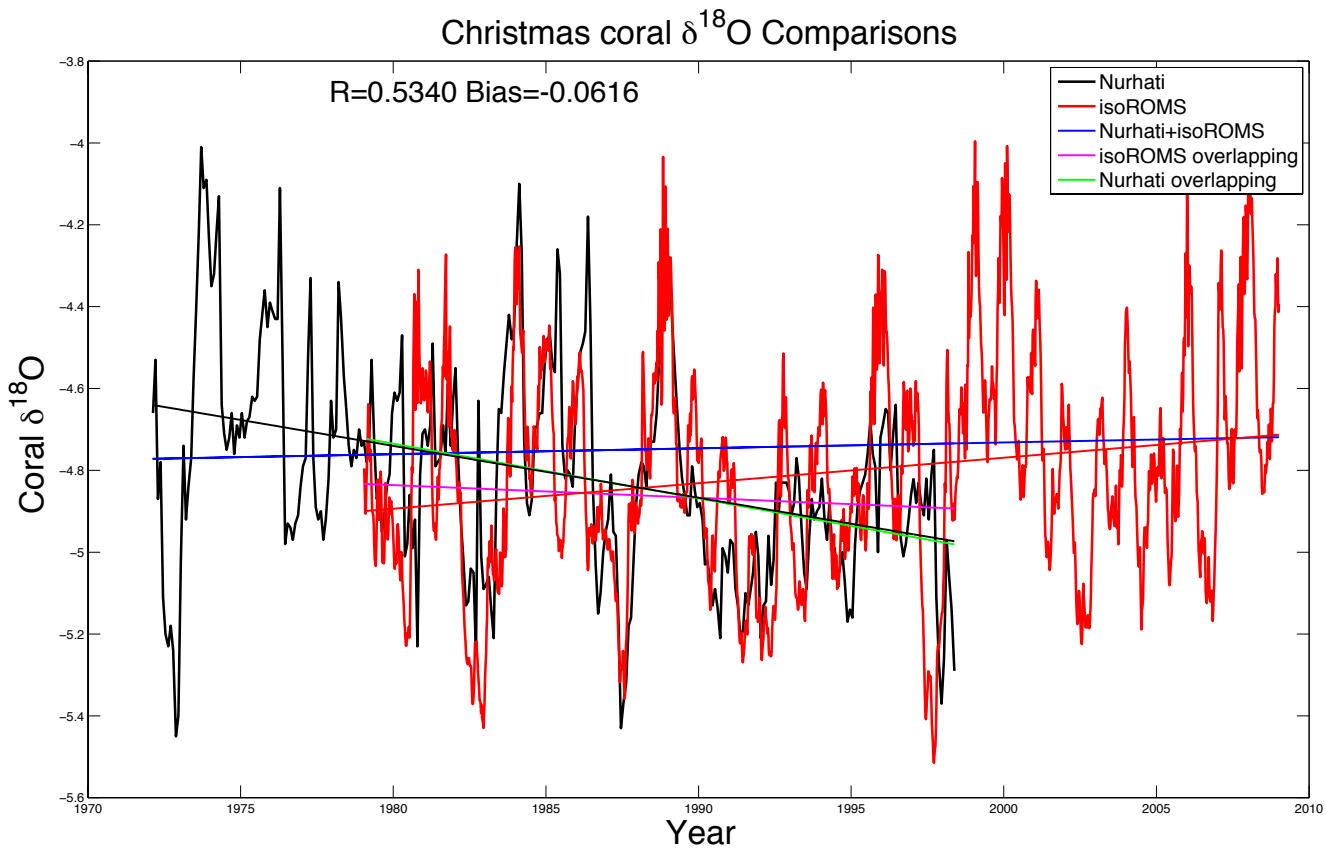

Figure 10. Christmas Island coral δ¹⁸O (‰) comparison.

-0.085(‰/20yr) and -0.028(‰/20yr) , for Christmas and Palmyra, respectively.

Fanning Island coral record extends until 2005, and trends in the overlapping

period are -0.16(‰/26yr) for coral $\delta^{18}O$ and 0.082(‰/26yr) for isoROMS.

Since the overlapping coral $\delta^{18}O$ trends compare well, the coral $\delta^{18}O$

record presented by Nurhati et. al (2009) can be extended using isoROMS coral

$\delta^{18}O$. This was done by adding isoROMS coral $\delta^{18}O$ from 1999-2009 for Palmyra

Atoll and Christmas Island, and from 2006-2009 for Fanning Island. Trends from

the combined coral $\delta^{18}O$ record are -0.098(‰/37yr), 0.033(‰/37yr), and

0.039(‰/37yr) for Palmyra Atoll, Fanning Island, and Christmas Island,

respectively, and are shown in Figures 8-10 by the blue trend line.

In order to look at spatial patterns across the Tropical Pacific, trend maps

were created using slopes from the linear regression for SST, SSS, and

thermocline depth. From these, the spatial trends can be observed, and

correlations of trend patterns inferred from coral $\delta^{18}O$ can be compared. Trend

maps were created for the overlapping period of 1979-1998, in order to simulate

as much of the Nurhati et. al (2009) study as possible and to validate the coral

proxies. The full model time period from 1979-2009 was also used, in order to

observe changes in the later time period.

Chapter 4: Results

      We use isoROMS to compare coral proxy records to Nurhati et. al (2009). Nurhati et. al (2009) claims that during the time period of 1972-1998, trends toward more negative coral $\delta^{18}O$ should be associated with warmer and wetter conditions. Nurhati et. al (2009) show that coral Sr/Ca SST proxies produce warming trends at all three Islands, ranging from 0.94 ± 5.81(°C/26yr) at Palmyra, to 1.37 ± 6.57(°C/26yr) at Fanning, to 1.65 ± 5.73(°C/26yr) at Christmas (Nurhati et. al, 2009). When disregarding the large uncertainties of Sr/Ca proxies, these agree with ERSST v.3b, with trends of 0.99(°C/26yr) at Palmyra, 1.11(°C/26yr) at Fanning, and 1.16(°C/26yr) at Christmas; however, the Sr/Ca ratios express a greater magnitude of warming near the equator than ERSST v.3b.
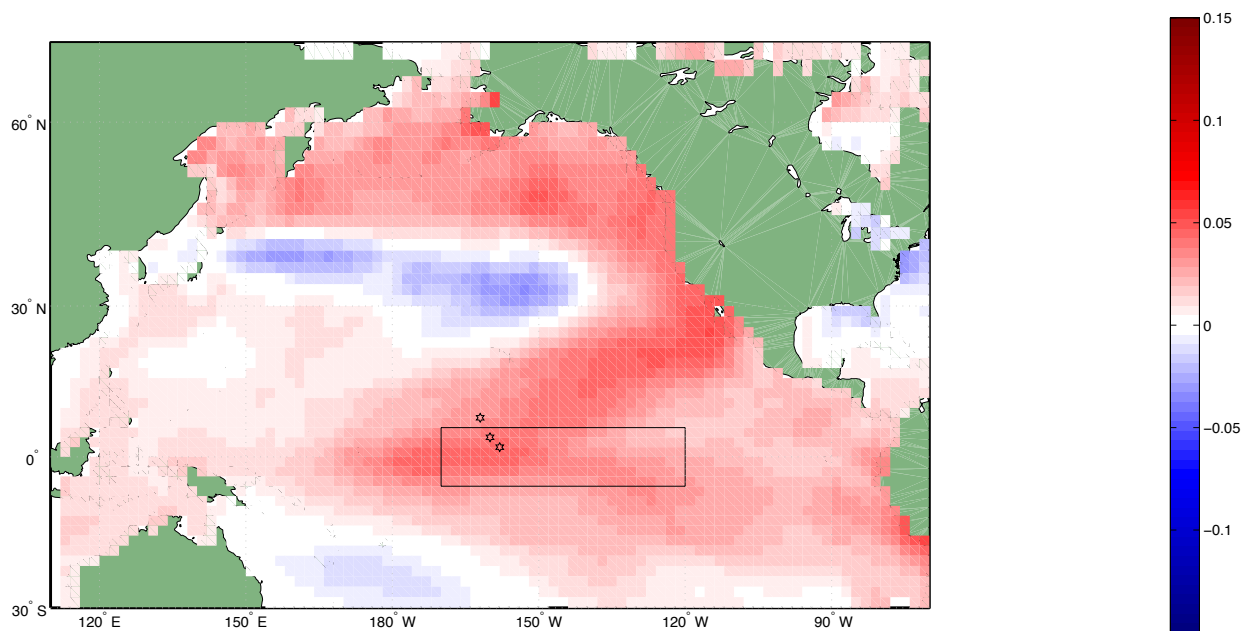

Figure 11. SST trends (°C/year) from ERSST v.3b from 1972-1998.

Warming trends during the Nurhati et. al (2009) time period in ERSST extend

throughout the equatorial Pacific (Figure 11) and look similar to a positive phase

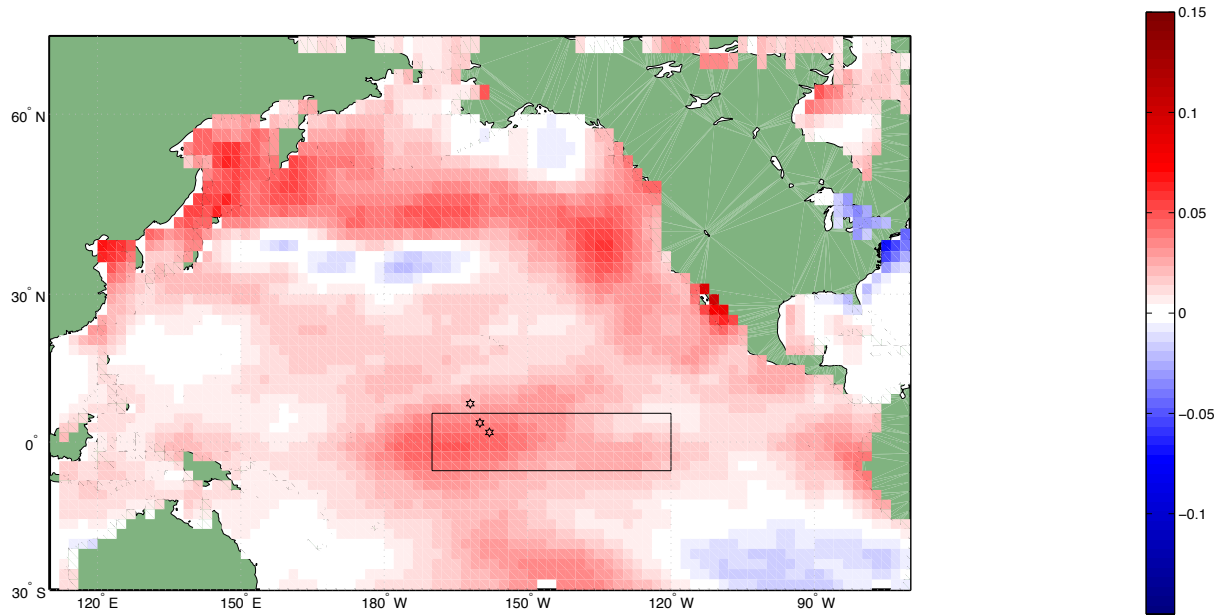of the Pacific Decadal Oscillation (PDO) SST distribution.   During the overlap

Figure 12. SST trends (°C/year) from ERSST v.3b from overlapping period 1979-1998.

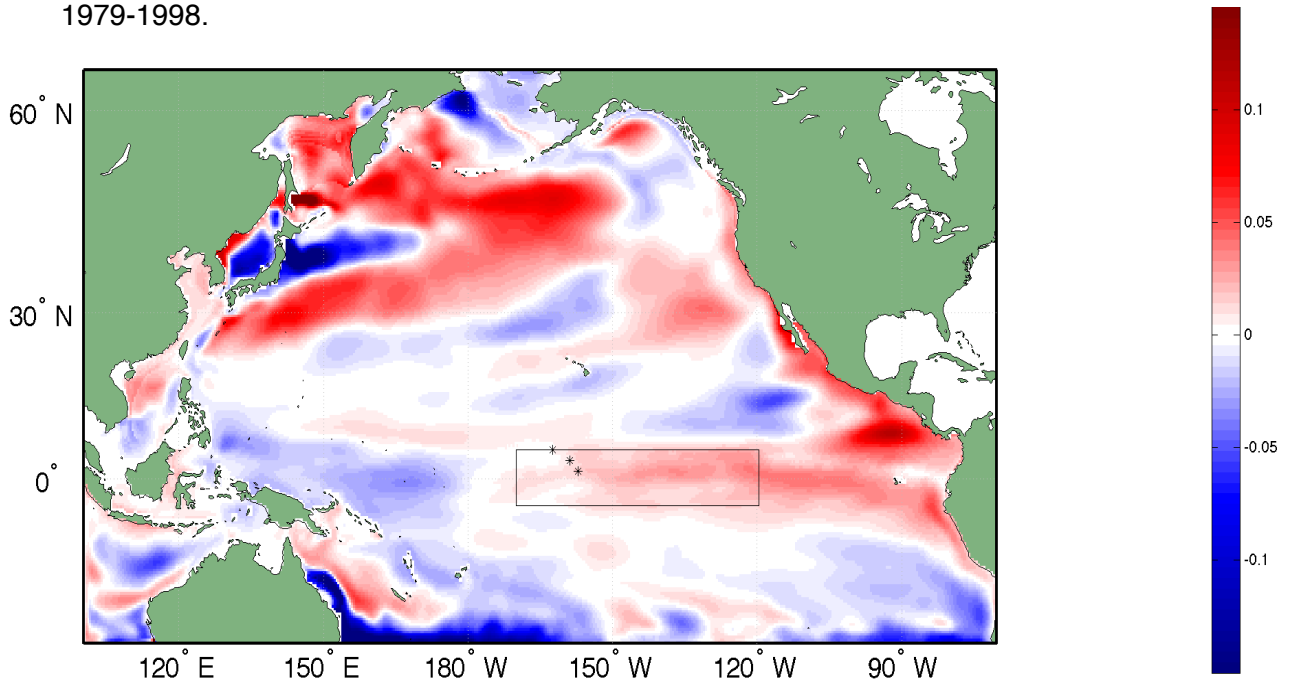Figure 13. Bulk (50m) SST trends (°C/year) from isoROMS from overlapping period 1979-1998.

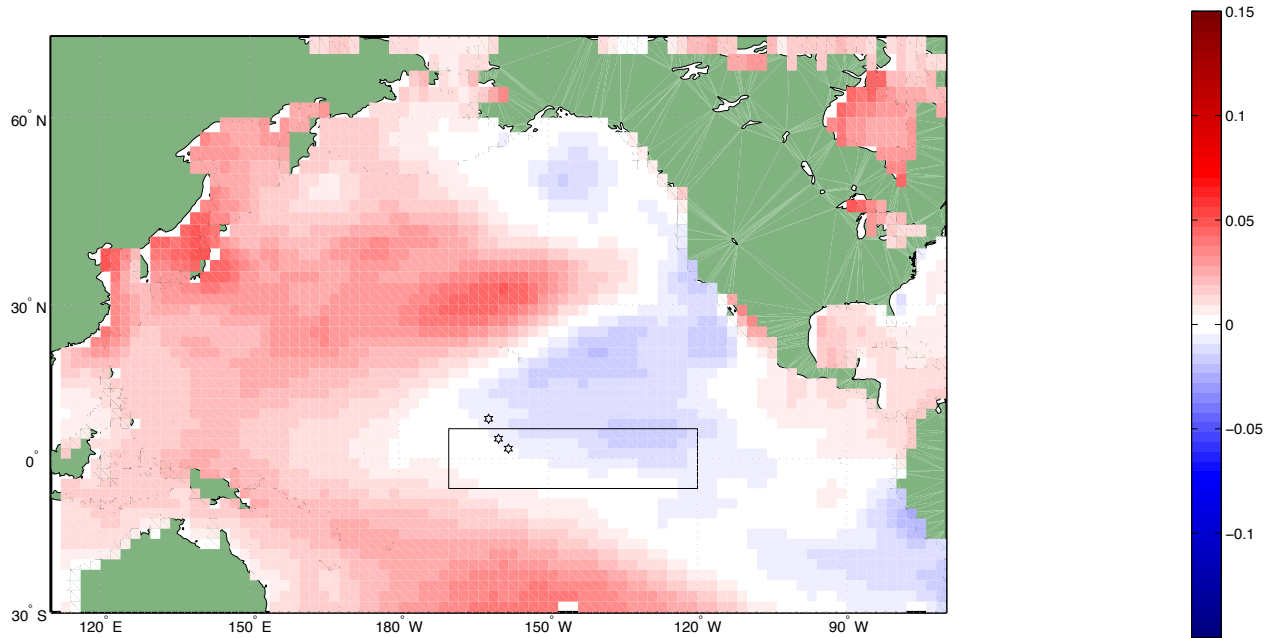Figure 14. SST trends (°C/year) from ERSST v.3b from extended period 1979-2009.
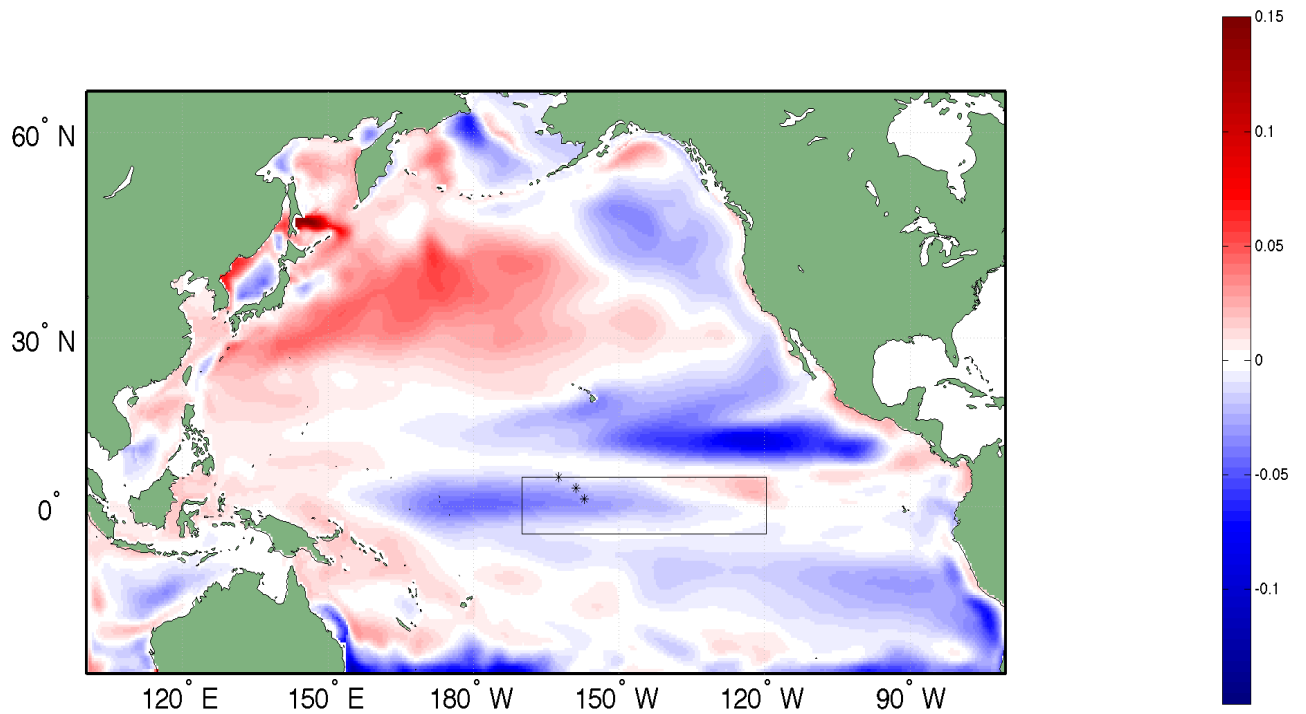

Figure 15. Bulk (50m) SST trends (°C/year) from isoROMS from extended period 1979-2009.

period (1979-1998), temperature trends from isoROMS agree with proxy trends in the Line Islands, with the strongest warming at the equator (Figures 8-10). The trends from the overlap period in Figure 12 and 13 show a reduced SST zonal gradient across the Tropical Pacific, which is opposite from 1979-2009 (Figure 14 and 15), which reveals a strengthening of the zonal SST gradient. From 1979-2009, isoROMS and ERSSTv.3b generally agree spatially, but with isoROMS showing more cooling in the western Pacific. In the Line Islands region, both ERSSTv.3b and isoROMS show cooling trends, which corresponds to the increase in coral $\delta^{18}O$ as shown in isoROMS. As shown in Figures 8-10, the largest decrease in $\delta^{18}O$ was during the 1997-1998 El Niño event, but afterwords there was a restoration to more normal conditions. Nurhati et. al (2009) halted their analysis at the peak of this anomalous event.

For SSS trends, the $\delta^{18}O_{sw}$ trends from Nurhati et. al (2009) are compared with SSS trends from isoROMS and the gridded salinity data product from Delcroix et. al (2011). $\delta^{18}O$ seawater trends over 1972-1998 from Nurhati et. al (2009) for Palmyra, Fanning, and Christmas exhibit trends of -0.32 ± 0.08(‰/26yr), -0.12 ± 0.08(‰/26yr), 0.03 ± 0.11(‰26yr), respectively. If assuming a linear correlation between SSS and $\delta^{18}O_{sw}$, this would result in the largest freshening trends at Palmyra, smaller trends at Fanning, and no freshening trends at the southernmost Island Christmas. From 1972-1998, the Delcroix et. al (2011) data
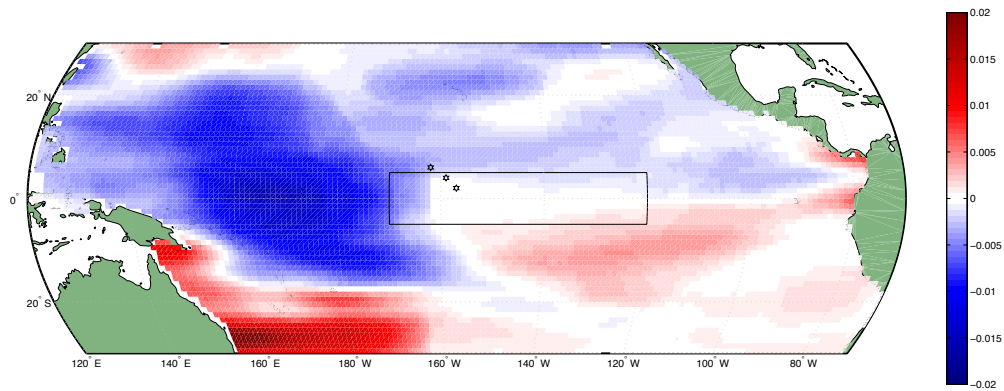
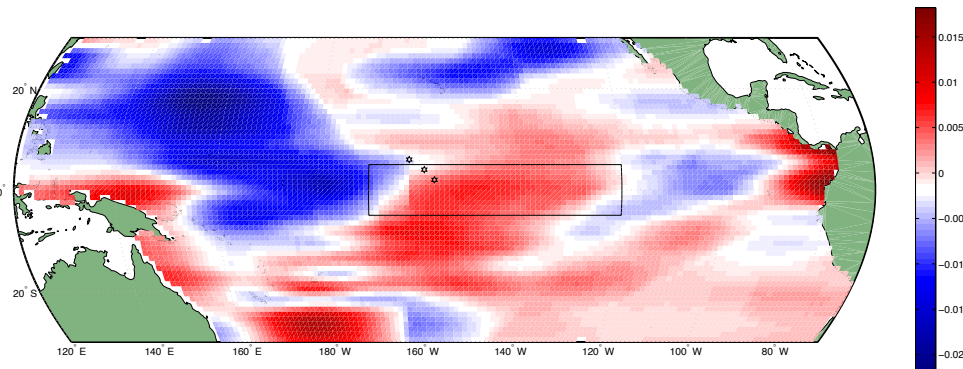Figure 16. SSS trends (psu/year) 1972-1998 from Delcroix et. al (2011) data set.

Figure 17. SSS trends (psu/year) 1979-1998 overlapping period, from Delcroix et. al (2011) data set.
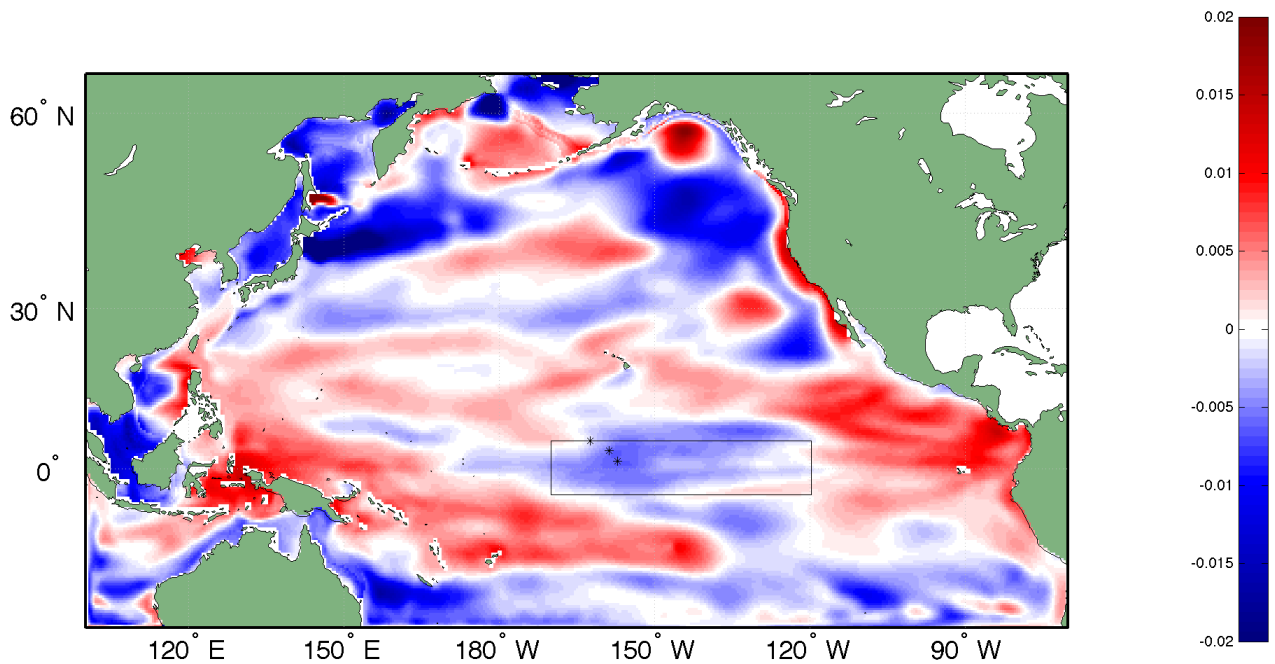

Figure 18. Bulk (50m) SSS trends (psu/year) 1979-1998 overlapping period, from isoROMS.

set show trends (Figure 16) that correspond with $\delta^{18}O_{sw}$ trends, and also show

the Western Pacific trending towards lower salinities. During the overlapping

time period of 1979-1998, Delcroix et. al (2011) (Figure 17) and isoROMS (Figure

18) show opposite patterns in the Line Islands region. IsoROMS exhibits the

opposite trends that would be expected from the $\delta^{18}O_{sw}$ trends. IsoROMS a trend
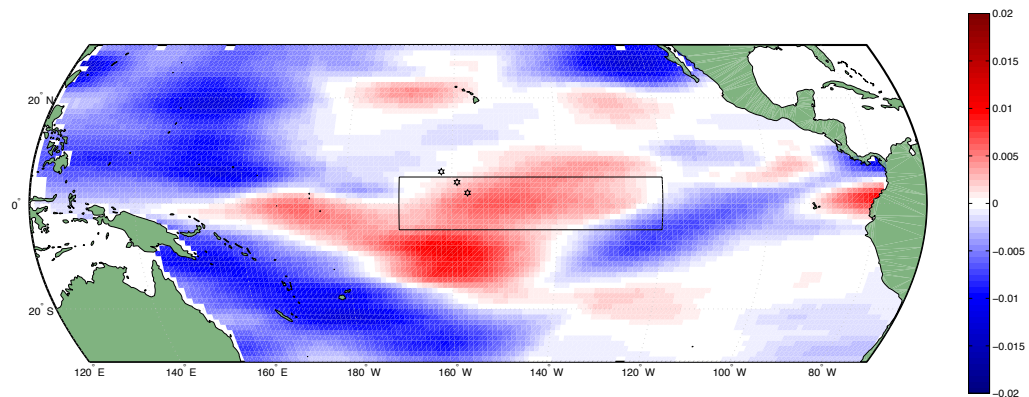

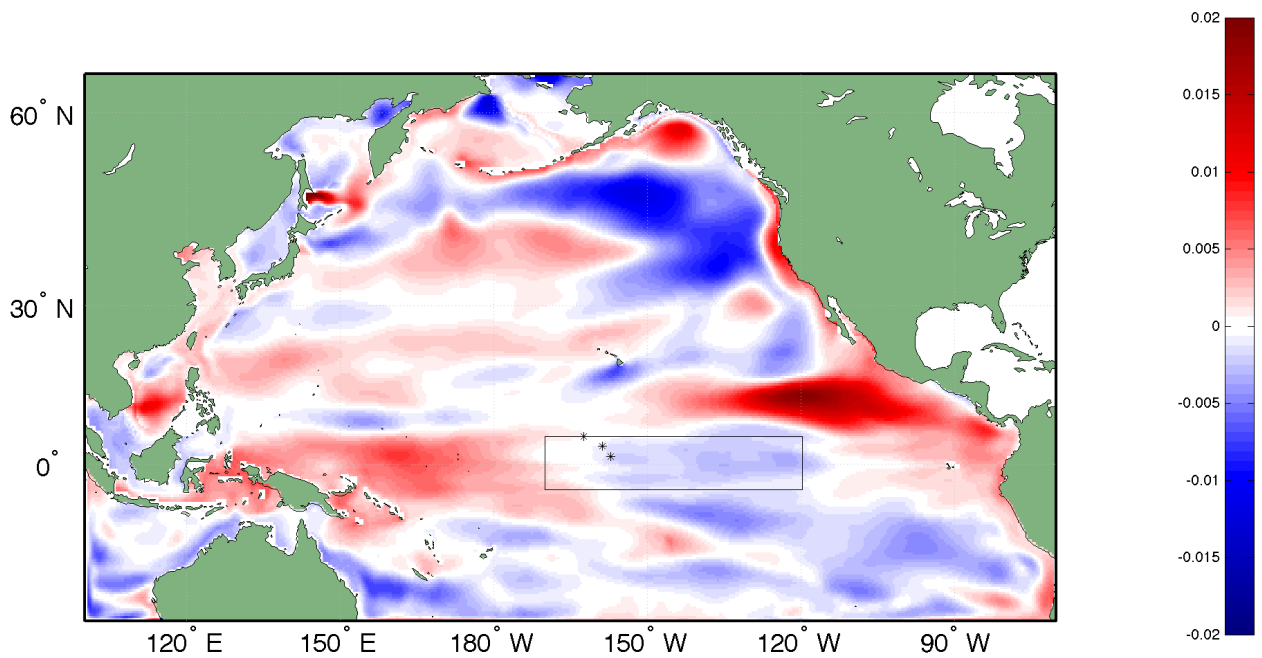Figure 19. SSS trends (psu/year) 1979-2009 extended period, from Delcroix et. al (2011) data set.

Figure 20. Bulk (50m) SSS trends (psu/year) 1979-2009 extended period, from isoROMS.

towards saltier water despite having a similar $\delta^{18}O$ trend. If only using isoROMS

for salinity trends, this would be an indication that the $\delta^{18}O_{sw}$ and SSS

relationship is not consistent with the interpretation of a linear proxy. Trends

from Delcroix et. al (2011) agree spatially with the $\delta^{18}O_{sw}$ records, which suggests

that the role of salinity in $\delta^{18}O$ in not nearly as significant as previously thought.

During the isoROMS period of 1979-2009, SST and SSS trends in isoROMS

are very dissimilar to those of the Nurhati period, from 1972-1998.   Expanding

the data by another decade shows very different patterns, and is also represented

as changes in isoROMS coral $\delta^{18}O$. The trends for the common period between

the Nurhati time period and isoROMS time period are similar, and towards the

end of the isoROMS period, the coral $\delta^{18}O$ trends in the positive direction

(Figures 8-10), which is a result of a fundamental shift in the Pacific after the

large 1997-1998 El Niño.

Thermocline trends are directly related to wind forcing and can show the

dynamics at play in the equatorial region. From the warming trends that

increased towards the equator, Nurhati et. al (2009) suggested a decrease in

equatorial upwelling from 1972-1998. However, for the overlapping period of

1979-2009, no trends in equatorial upwelling are present at the equator in

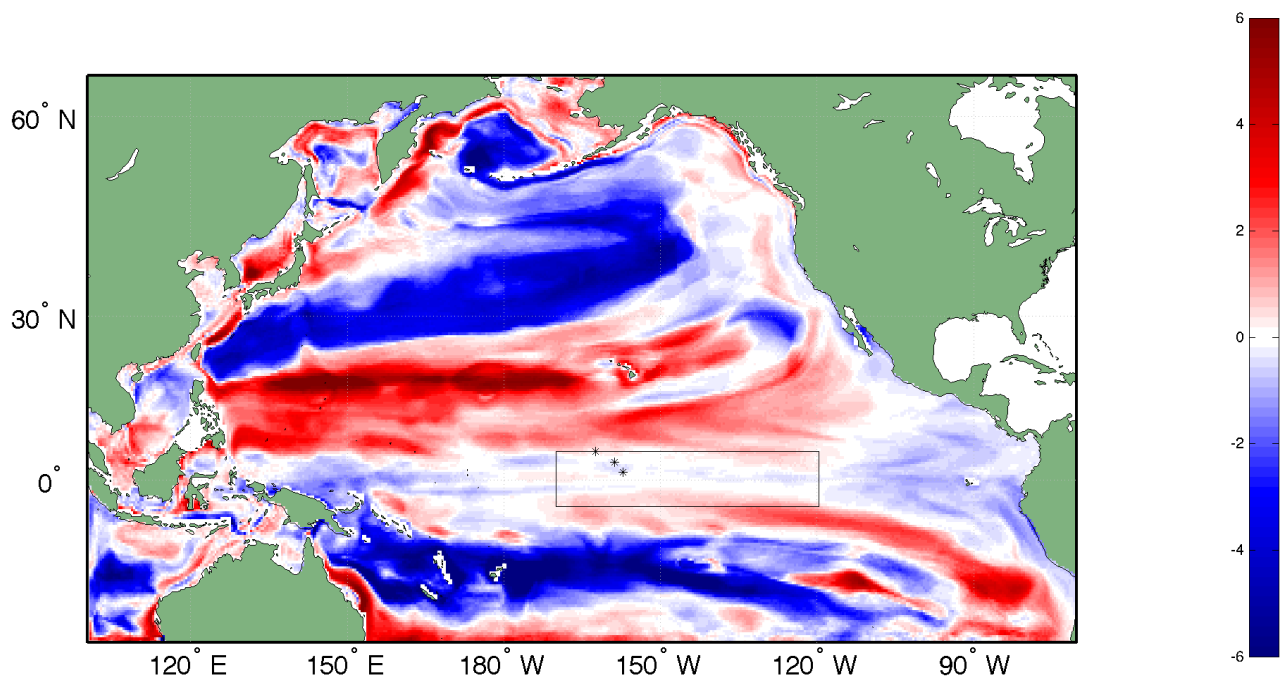isoROMS (Figure 21), contrary to what Nurhati et. al (2009) suggest. McPhaden

Figure 21. Thermocline depth trends (meters/year) from isoROMS for overlapping period 1979-1998. Red indicates shoaling and blue deepening of the thermocline.
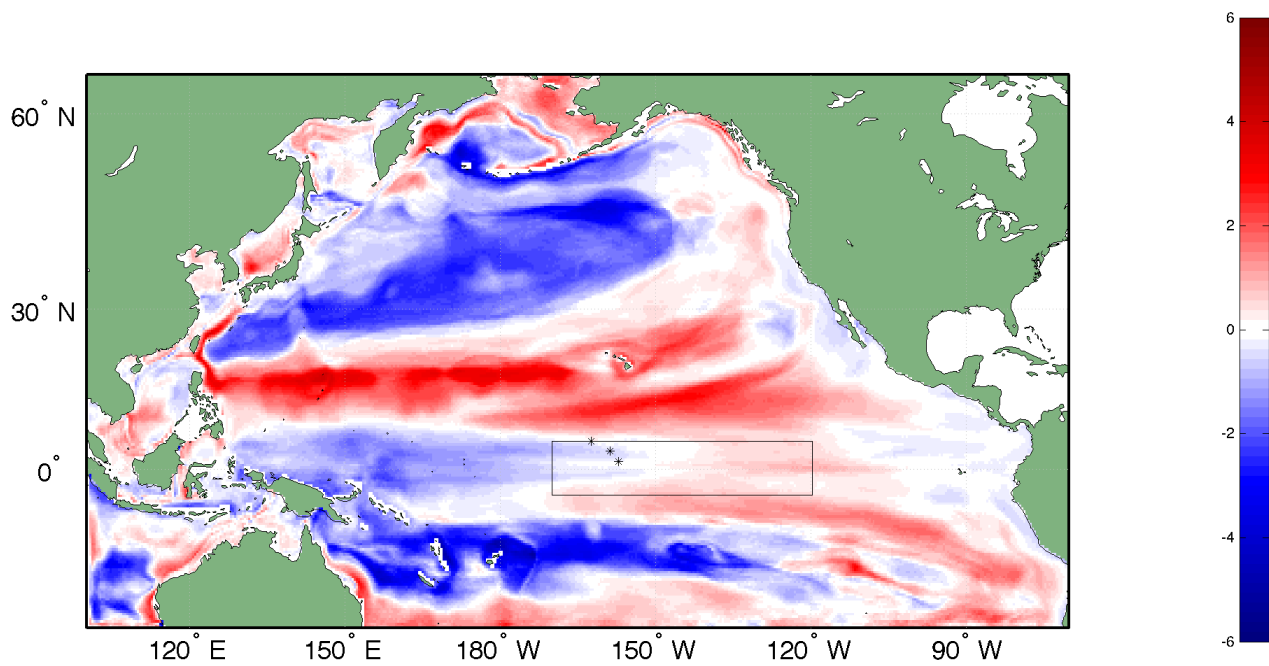

Figure 22. Thermocline depth trends (meters/year) from isoROMS for extended period 1979-2009.

and Zhang (2002) has shown that there has been a reduction in equatorial upwelling since the 1970's, associated with a weakened meridonal atmospheric circulation; however, these trends are not seen with isoROMS (Figure 22). For the extended time period, the thermocline trend pattern near the equator is a typical "La Niña like" pattern, with enhanced upwelling in the Eastern Pacific, and trends towards a deeper thermocline in the Western Pacific. The extended period, mainly after 1998, experienced a strengthening of easterly trade winds (Merrifield & Maltrud, 2011), and is seen in the extended isoROMS period for thermocline trends. For both the overlapping and the extended time period, thermocline trends in the subtropics and mid-latitudes are much more robust compared to the equatorial region, but they are not investigated in this study.

This study also shows the importance of time period selection, especially when computing trends from relatively short time frames, or time frames in which a decadal or multi-decadal oscillation may dominate. Nurhati et. al (2009) show strong negative trends in coral $\delta^{18}O$ from 1972-1998, which were unprecedented in the last century. However, when isoROMS coral $\delta^{18}O$ data is added to the data sets of Nurhati et. al (2009), at both Christmas and Fanning, trends becomes positive, while Palmyra is still negative, albeit with a lower magnitude. While it is important to quantify anomalous trends and their causes, longer trends are needed to observe changes to the climate system.

Using isoROMS, the relationship between SSS and $\delta^{18}O_{sw}$ can be studied in great detail, as isoROMS presents SSS and $\delta^{18}O_{sw}$ datasets which are complete in space and time. The correlation plots (Figure 23) for the Line Islands are compared, and the substantial scatter in the relationship is seen. When investigating further, linear relations tend to develop during strong El Niño events, and non-linear relations prevail for the majority of the time.
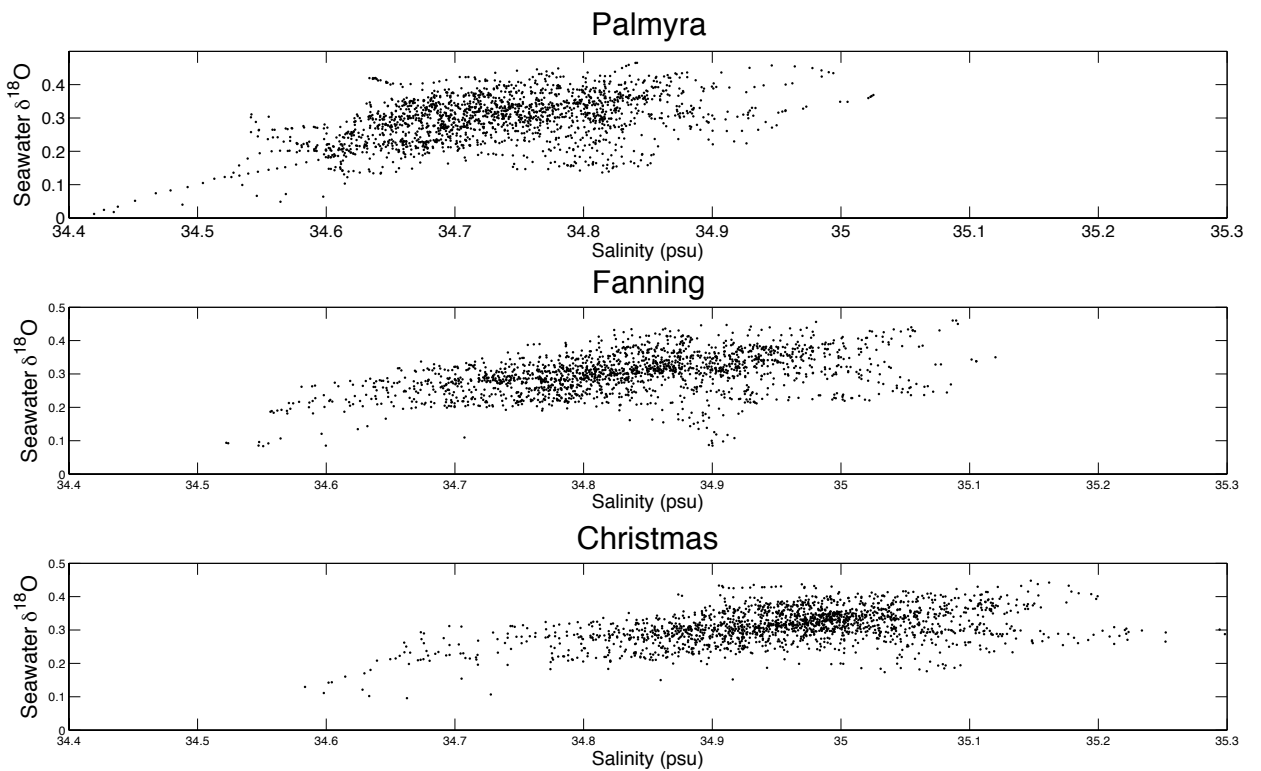

Figure 23. Correlation between SSS (psu) and $\delta^{18}O_{sw}$ (‰) in the Line Islands.

Chapter 5: Conclusion

Coral $\delta^{18}O$, which is a function of temperature and the $\delta^{18}O$ of the local

seawater, is a suitable proxy for reconstructing the ENSO system in the tropical

Pacific Ocean. Errors arise when assuming that $\delta^{18}O_{sw}$ is linearly correlated with

sea surface salinity. In the late twentieth century Nurhati et. al (2009) found

strong negative coral $\delta^{18}O$ trends from the time period of 1972-1998 in corals

from the Line Islands in the Central Tropical Pacific. From the coral Sr/Ca

records, Nurhati et. al (2009) inferred warming trends that increase towards the

equator and suggest a decrease in equatorial upwelling. Using the residual

$\delta^{18}O_{sw}$ record, more negative trends were observed in the northern-most Island,

Palmyra, and Nurhati et. al (2009) associate this with an equatorward

strengthening/shift of the ITCZ. Using a numerical model, it is possible to

examine how Line Islands coral $\delta^{18}O$ explains changes in the region. Coral

records and isoROMS agree in warming trends, but isoROMS does not suggest a

decrease in equatorial upwelling thought to be associated with the enhanced

equatorial warming. $\delta^{18}O_{sw}$ records and SSS from isoROMS disagree spatially,

with opposite meridonal trends. This may be a result of the nonlinearity

between $\delta^{18}O_{sw}$ and SSS, which has implications for interpreting coral $\delta^{18}O$

records. It is important to note that this could also be due to uncertainties with

salinity data, with salinity trends from the Delcroix et. al (2011) data set agreeing spatially with the $\delta^{18}O_{sw}$ trends.

This study also shows the importance of time period selection when studying time-series data, and how relatively short time periods for computing trends are more associated with decadal oscillations than with long term trends. The late twentieth century is distinct compared to the entire twentieth century (Nurhati et. al, 2009), and changes are in line with the leading global warming hypothesis for the tropical Pacific (Collins et. al, 2010). However, changes to the mean state need much longer timescales to be verified. Periods of 20-30 years are more likely to be associated with decadal oscillations, such as the Pacific Decadal Oscillation. This is observed in the model, when the time period of Nurhati et. al (2009) study is extended to 2009, the strong negative coral $\delta^{18}O$ trends disappear. Changes in the entire Tropical Pacific are also observed, and show that this region has changed dramatically after the time frame of the study by Nurhati et. al (2009). This study also recognizes the ability of regional ocean models to validate past ocean conditions with collected proxy data and provide contextual spatial trends that single proxy time-series cannot. Coral $\delta^{18}O$ is a suitable proxy for ENSO variability, albeit with some limitations. As discussed in this study, but not investigated, the non-linearity between $\delta^{18}O_{sw}$ and sea surface salinity inherently makes the interpretation of past climate more complex, and should be

addressed in the future. Longer term anthropogenic signals and decadal

variability can be separated by studying longer time frames, as shorter time

frames (20-30 years) can show significant non-climate variability.

References:

Carilli, J. E., H. V. McGregor, J. J. Gaudry, S. D. Donner, M. K. Gagan, S. Stevenson, H. Wong, and D. Fink (2014), Equatorial Pacific coral geochemical records show recent weakening of the Walker Circulation, Paleoceanography, 29, 1031–1045, doi:10.1002/ 2014PA002683.

Cobb, K. M., Charles, C. D., Cheng, H., & Edwards, R. L. (2003). El Nino/ Southern Oscillation and tropical Pacific climate during the last millennium. Nature, 424(6946), 271-276.

Collins, M., An, S. I., Cai, W., Ganachaud, A., Guilyardi, E., Jin, F. F., ... & Wittenberg, A. (2010). The impact of global warming on the tropical Pacific Ocean and El Niño. Nature Geoscience, 3(6), 391-397.

Conroy, J. L., Cobb, K. M., Lynch-Stieglitz, J., & Polissar, P. J. (2014). Constraints on the salinity–oxygen isotope relationship in the central tropical Pacific Ocean. Marine Chemistry, 161, 26-33.

Delcroix,T., G. Alory, S. Cravatte, T. Correge, and M. McPhaden, (2011). A gridded sea surface salinity data set for the tropical Pacific with sample applications (1950-2008). Deep Sea Res., 58, 38-48 doi:10.1016/j.dsr. 2010.11.002″

England, M. H., McGregor, S., Spence, P., Meehl, G. A., Timmermann, A., Cai, W.,

    ... & Santoso, A. (2014). Recent intensification of wind-driven circulation in

    the Pacific and the ongoing warming hiatus. Nature Climate change, 4(3),

    222-227.

Grottoli, A. G., & Eakin, C. M. (2007). A review of modern coral δ 18 O and Δ 14

    C proxy records. Earth-Science Reviews, 81(1), 67-91.

Held, I. M., & Soden, B. J. (2006). Robust responses of the hydrological cycle to

    global warming. Journal of Climate, 19(21), 5686-5699.

Karnauskas, K. B., Seager, R., Kaplan, A., Kushnir, Y., & Cane, M. A. (2009).

    Observed strengthening of the zonal sea surface temperature gradient

    across the equatorial Pacific Ocean*. Journal of Climate, 22(16), 4316-4321.

LeGrande, A. N., & Schmidt, G. A. (2006). Global gridded data set of the oxygen

    isotopic composition in seawater. Geophysical Research Letters, 33(12).

LeGrande, A. N., & Schmidt, G. A. (2011). Water isotopologues as a quantitative

    paleosalinity proxy. Paleoceanography, 26(3).

McPhaden, M. J., Busalacchi, A. J., Cheney, R., Donguy, J. R., Gage, K. S., Halpern,

    D., ... & Takeuchi, K. (1998). The Tropical Ocean–Global Atmosphere

observing system: A decade of progress. Journal of Geophysical Research: Oceans (1978–2012), 103(C7), 14169-14240.

McPhaden, M. J., & Zhang, D. (2002). Slowdown of the meridional overturning circulation in the upper Pacific Ocean. Nature, 415(6872), 603-608.

Merrifield, M. A., & Maltrud, M. E. (2011). Regional sea level trends due to a Pacific trade wind intensification. Geophysical Research Letters, 38(21).

Nurhati, I.S., K.M. Cobb, C.D. Charles, and R.B. Dunbar. (2009). Late 20th century warming and freshening in the central tropical Pacific. Geophys. Res. Lett., 36, L21606

Russon, T., Tudhope, A. W., Hegerl, G. C., Collins, M., & Tindall, J. (2013). Inter-annual tropical Pacific climate variability in an isotope-enabled CGCM: implications for interpreting coral stable oxygen isotope records of ENSO. Climate of the Past, 9(4), 1543-1557.

Shchepetkin, A. F., & McWilliams, J. C. (2005). The regional oceanic modeling system (ROMS): a split-explicit, free-surface, topography-following-coordinate oceanic model. Ocean Modelling, 9(4), 347-404.

Smith, T., R. W. Reynolds, T. C. Peterson, and J. Lawrimore, 2008: Improvements to NOAA's historical merged land-ocean surface temperature analysis (1880-2006). J. Climate, 21, 2283–2296.

Stevenson, S., B. Fox-Kemper, M. Jochum, R. Neale, C. Deser, and G. Meehl, 2012: Will there be a significant change to El Nino in the 21st century? Journal of Climate, 25, 2129–2145, CCSM4 special issue. doi:10.1175/ JCLI-D-11-00252.1.

Stevenson, S., H. V. McGregor, S. Phipps, and B. Fox-Kemper. (2013). Quantifying Errors in Coral-based ENSO Estimates: Towards Improved Forward Modeling of δ^{18}O. Paleoceanography, 28, 1–17, doi:10.1002/palo.20059.

Stevenson, S., Powell, B., Merrifield, M., Cobb, K.,Nusbaumer, J. & Noone, D. (2015). Characterizing Coral Proxy Environments for Improved Climate Reconstruction: Mesoscale Influences on Central Pacific Islands.

Stevenson, S., Fox-Kemper, B., Jochum, M., Rajagopalan, B., & Yeager, S. G. (2010). ENSO model validation using wavelet probability analysis. Journal of Climate, 23(20), 5540-5547.

Urban, Frank E., Julia E. Cole, and Jonathan T. Overpeck. "Influence of mean climate change on climate variability from a 155-year tropical Pacific coral record." Nature 407.6807 (2000): 989-993.

Vecchi, G. A., Soden, B. J., Wittenberg, A. T., Held, I. M., Leetmaa, A., & Harrison, M. J. (2006). Weakening of tropical Pacific atmospheric circulation due to anthropogenic forcing. Nature, 441(7089), 73-76.